

# Independent variations of CH<sub>4</sub> emissions and isotopic composition over the past 160,000 years

Lars Möller<sup>1,2</sup>, Todd Sowers<sup>3</sup>, Michael Bock<sup>2</sup>, Renato Spahni<sup>2</sup>, Melanie Behrens<sup>1</sup>, Jochen Schmitt<sup>2</sup>, Heinrich Miller<sup>1</sup> and Hubertus Fischer<sup>1,2\*</sup>

**During the last glacial cycle, greenhouse gas concentrations fluctuated on decadal and longer timescales. Concentrations of methane, as measured in polar ice cores, show a close connection with Northern Hemisphere temperature variability, but the contribution of the various methane sources and sinks to changes in concentration is still a matter of debate. Here we assess changes in methane cycling over the past 160,000 years by measurements of the carbon isotopic composition  $\delta^{13}\text{C}$  of methane in Antarctic ice cores from Dronning Maud Land and Vostok. We find that variations in the  $\delta^{13}\text{C}$  of methane are not generally correlated with changes in atmospheric methane concentration, but instead more closely correlated to atmospheric CO<sub>2</sub> concentrations. We interpret this to reflect a climatic and CO<sub>2</sub>-related control on the isotopic signature of methane source material, such as ecosystem shifts in the seasonally inundated tropical wetlands that produce methane. In contrast, relatively stable  $\delta^{13}\text{C}$  values occurred during intervals of large changes in the atmospheric loading of methane. We suggest that most methane sources—most notably tropical wetlands—must have responded simultaneously to climate changes across these periods.**

Climate variations over the past glacial cycle are characterized by global temperature changes<sup>1,2</sup>, sea-level fluctuations<sup>3,4</sup> and substantial changes in atmospheric greenhouse gas concentrations<sup>5</sup>. Abrupt climate shifts, for example Dansgaard–Oeschger events, characterize much of the glacial records in the Northern Hemisphere and are mirrored in the ice-core CH<sub>4</sub> record<sup>6,7</sup>.

The nature of the CH<sub>4</sub>–climate coupling on glacial–interglacial and millennial timescales is still a matter of debate<sup>7,8</sup>. Studies of the inter-polar CH<sub>4</sub> concentration difference using ice cores from both polar regions are interpreted as a constraint of the latitudinal distribution of CH<sub>4</sub> emission sources<sup>9,10</sup>. Furthermore, most CH<sub>4</sub> sources/sinks have characteristic isotope signatures. Accordingly, atmospheric CH<sub>4</sub> isotope records provide refined boundary conditions to constrain changes in individual sources or sinks over time<sup>11–13</sup>. Here we present CH<sub>4</sub> isotope data from ice cores covering the past 160,000 years (160 kyr; Fig. 1), thereby extending the atmospheric  $\delta^{13}\text{CH}_4$  record to a full glacial–interglacial cycle.

Generally, our record confirms increased  $\delta^{13}\text{CH}_4$  values under full glacial conditions<sup>11</sup>, decreasing  $\delta^{13}\text{CH}_4$  during terminations (except during the unique Younger Dryas cold reversal) and the continuation of this declining trend over the following interglacial<sup>13</sup>, irrespective of the CH<sub>4</sub> evolution. Although an unambiguous alignment of termination I and II is not possible owing to the Younger Dryas event,  $\delta^{13}\text{CH}_4$  values of the two deglaciations seem to be offset by  $\sim 2\%$  (Fig. 2). Minimum  $\delta^{13}\text{CH}_4$  values are found during marine isotope stage (MIS) 5d–e.  $\delta^{13}\text{CH}_4$  increases over the past glaciation, superimposed by variability largely in parallel to millennial CO<sub>2</sub> changes. Most importantly, this new  $\delta^{13}\text{CH}_4$  record does not share common features with the CH<sub>4</sub> record over the same interval. The most striking of these dissimilarities is found during the MIS 5–4 transition (between 70

and 64 kyr before present (BP), where present is defined as 1950), when  $\delta^{13}\text{CH}_4$  rises by  $\sim 4\%$ , whereas CH<sub>4</sub> fluctuations are smaller than 50 parts per 10<sup>9</sup> (ppb; Fig. 3). In stark contrast to the MIS 5–4 transition, rapid CH<sub>4</sub> changes during Dansgaard–Oeschger events are not imprinted in the  $\delta^{13}\text{CH}_4$  record.

Comparing the full  $\delta^{13}\text{CH}_4$  record with other global climate records provides some surprising insights into the CH<sub>4</sub>/ $\delta^{13}\text{CH}_4$  system (Fig. 1): correlations of our  $\delta^{13}\text{CH}_4$  record with CH<sub>4</sub>, sea level and CO<sub>2</sub> data lead to correlation coefficients ( $R^2$ ) of 0.29, 0.47 and 0.74, respectively. Moreover,  $\delta^{13}\text{CH}_4$  and CO<sub>2</sub> are not only correlated on the glacial–interglacial timescale, but also over millennial scale variations associated with the Antarctic Isotope Maxima<sup>2,14</sup>.

In summary, the decoupling of CH<sub>4</sub> loading and  $\delta^{13}\text{CH}_4$  can be separated into two general phenomena: times when CH<sub>4</sub> source/sink variations change the atmospheric loading with little or no imprint in  $\delta^{13}\text{CH}_4$ ; and times when  $\delta^{13}\text{CH}_4$  varies substantially but the balance of sources and sinks, thus CH<sub>4</sub> concentration, seems to be rather constant. We will discuss the  $\delta^{13}\text{CH}_4$  record in two parts, based on these two surprising observations.

## Rapid CH<sub>4</sub> concentration changes

The mean carbon isotopic signature of atmospheric CH<sub>4</sub> represents a flux weighted mean of all source emissions shifted by the isotopic fractionation induced by its sinks<sup>15</sup>. We can think of several explanations for periods where CH<sub>4</sub> loading changed, but  $\delta^{13}\text{CH}_4$  remained effectively constant. Given that the primary sink for atmospheric CH<sub>4</sub> is OH oxidation (>85%), changes in the palaeo OH reaction rates would influence the loading through changes in lifetime, but leave  $\delta^{13}\text{CH}_4$  unchanged. We discount this possibility based on atmospheric chemical modelling studies that show only subtle changes (<20%) in OH sink strength during glacial

<sup>1</sup>Alfred Wegener Institute, Helmholtz Centre for Polar and Marine Research, Am Alten Hafen 26, 27568 Bremerhaven, Germany, <sup>2</sup>Climate and Environmental Physics, Physics Institute & Oeschger Centre for Climate Change Research, University of Bern, Sidlerstrasse 5, 3012 Bern, Switzerland, <sup>3</sup>Pennsylvania State University, University Park, Pennsylvania 16802, USA. \*e-mail: hubertus.fischer@climate.unibe.ch

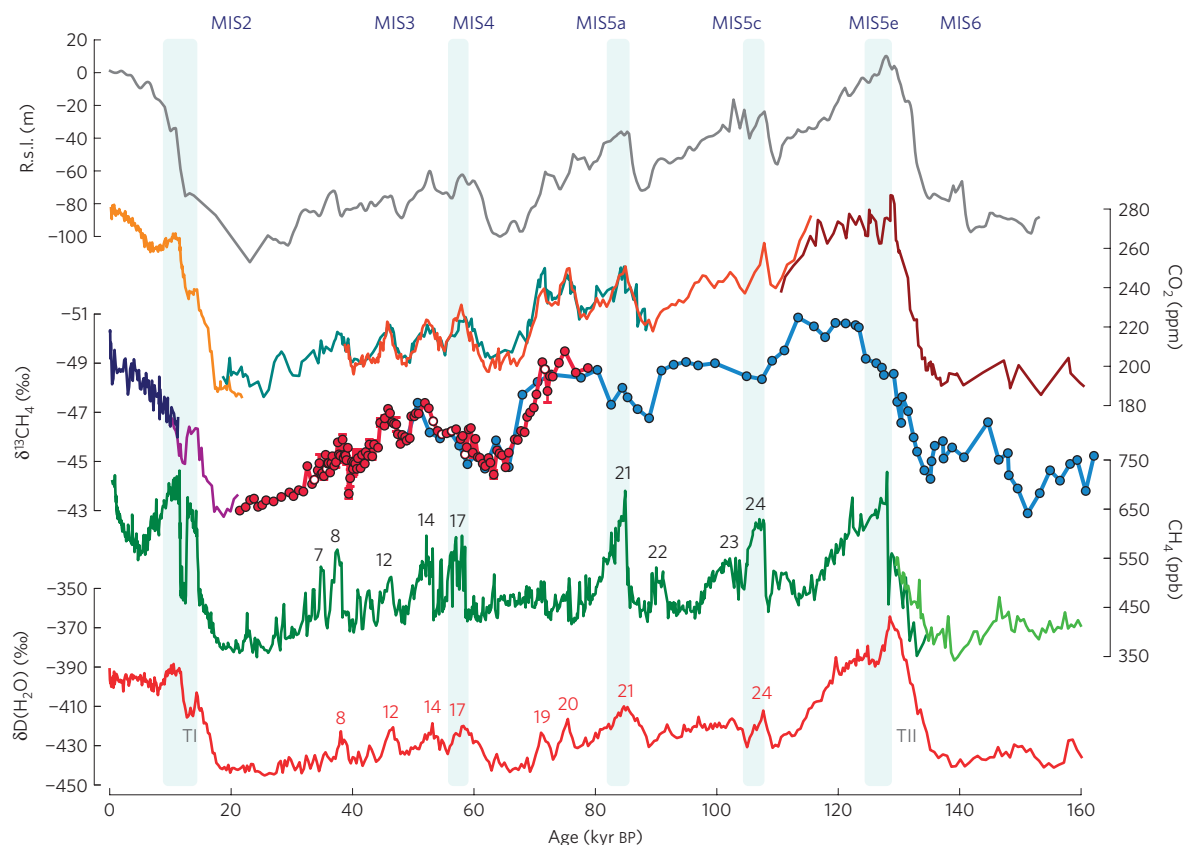


**Figure 1 | Methane carbon isotope and other climate records.** From top: relative sea-level (r.s.l.) reconstruction<sup>3,4</sup>. Atmospheric CO<sub>2</sub> from Vostok<sup>47</sup> (brown), EDML and Talos Dome<sup>48</sup> (orange), Byrd<sup>14</sup> (turquoise) and EPICA Dome C (EDC; ref. 49; yellow), in parts per million (ppm).  $\delta^{13}\text{CH}_4$  from Vostok (light blue) and EDML (dark red). Records for termination 1 (TI; ref. 11; EDML, purple) and the Holocene (Greenland Ice Sheet Project Two (GISP2), dark blue). Note the inverted y axis for the  $\delta^{13}\text{CH}_4$  records. Samples potentially affected by diffusive fractionation are marked by white circle fillings. Atmospheric CH<sub>4</sub> from EDC (ref. 7; light green) and EDML (ref. 5; dark green).  $\delta\text{D}$  in precipitation at Dome C (ref. 50; red). Arabic numbers indicate the timing of Dansgaard-Oeschger events and their respective Antarctic counterparts<sup>1,2</sup>. All records, except GISP2  $\delta^{13}\text{CH}_4$  and r.s.l., are given on the unified ice-core chronology<sup>46</sup>. Vertical bars indicate periods when the correlation between CO<sub>2</sub> and CH<sub>4</sub> breaks down. TII, termination 2.

periods<sup>16,17</sup>. We note however that the lifetime estimate is somewhat uncertain owing to the lack of accurate reconstructions for glacial NO<sub>x</sub> and volatile organic carbon concentrations, which influence tropospheric OH levels.

Alternatively, rapid Dansgaard-Oeschger CH<sub>4</sub> variability without a corresponding imprint in  $\delta^{13}\text{CH}_4$  could imply an almost proportional scaling of the main sources, causing the atmospheric  $\delta^{13}\text{CH}_4$  signature to remain relatively stable. Several lines of evidence suggest that this was the case. The latitudinal position of the intertropical convergence zone and the associated main monsoon systems are intimately coupled to Dansgaard-Oeschger climate variability<sup>6,18–21</sup>. Hydrological changes in low latitudes and their primary control on waxing and waning of tropical wetland emissions are arguably the most important factors driving glacial CH<sub>4</sub> emissions<sup>6,18</sup>. As the isotopic signature of tropical wetland emissions is closest to the mean  $\delta^{13}\text{CH}_4$  signature of all sources, changes in their emissions have only little impact on atmospheric  $\delta^{13}\text{CH}_4$ .

Palaeofire reconstructions inferred from charcoal records suggest increasing wildfire activity during interstadial periods<sup>22</sup>, although they do not allow for a quantitative estimate of wildfire CH<sub>4</sub> emissions. Wildfire emissions have the strongest leverage on the atmospheric  $\delta^{13}\text{CH}_4$  value, as its carbon isotopic signature is strongly enriched. Accordingly, the lack of considerable  $\delta^{13}\text{CH}_4$  shifts during Dansgaard-Oeschger events implies that increased wildfire emissions had to be compensated by another, isotopically light source. Combinations including additional <sup>13</sup>C-enriched wildfire emis-

sions during interstadials<sup>22</sup> and <sup>13</sup>C-depleted boreal permafrost emissions<sup>12,23,24</sup> could explain the observations, although it seems fortuitous that such relative changes would perfectly balance each other in all investigated events.

Enhanced emissions from high-latitude Northern Hemisphere CH<sub>4</sub> wetland sources (such as thermokarst lakes<sup>24</sup>, peatlands and permafrost thaw<sup>23</sup>, further denoted as boreal wetlands) have been suggested to explain increased inter-polar CH<sub>4</sub> gradients during interstadial periods<sup>9,10</sup>. Increased Northern Hemisphere CH<sub>4</sub> levels during interstadials, however, could also be caused by increased emissions from mid-to-low latitude wetland sources, for example, seasonally inundated floodplains in the Chinese lowlands, which are affected by expansive Asian summer monsoon rainfall<sup>21</sup>.

Finally, although geological CH<sub>4</sub> sources are thought to be slightly increased during glacial times owing to lowered sea levels<sup>25,26</sup>, they should be unaffected by Dansgaard-Oeschger events. Furthermore, large emissions from marine hydrates<sup>27</sup> during abrupt CH<sub>4</sub> episodes have been ruled out based on our recent  $\delta\text{D}(\text{CH}_4)$  ice-core studies<sup>12,28</sup>.

Possible sink configuration changes that could induce an equivalent enrichment in  $\delta^{13}\text{CH}_4$  to compensate for potential boreal CH<sub>4</sub> emissions would have to reduce the relative importance of the OH sink in the troposphere. However, owing to the expected reduction of volatile organic carbons during the glacial<sup>29,30</sup> and the feedback of lower CH<sub>4</sub> concentrations on the atmospheric OH concentration itself, the OH sink was probably even more important during cold conditions. In summary, a strong feedback of the main monsoon

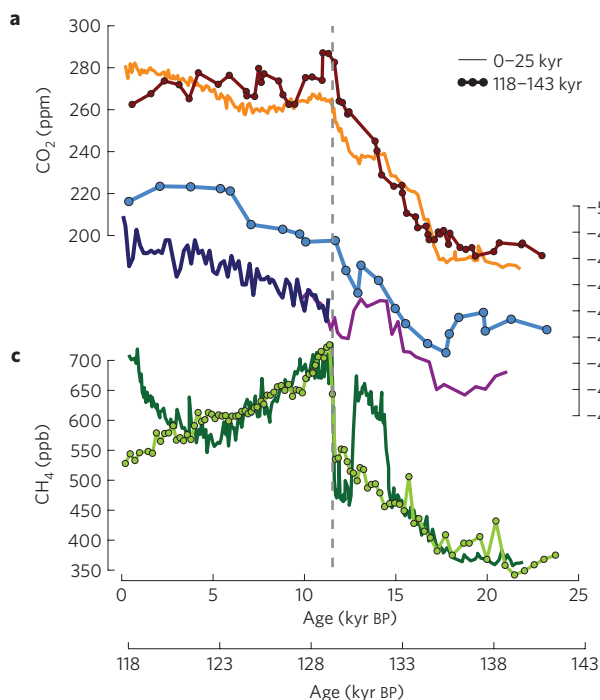


**Figure 2 | Climate conditions during the ultimate and penultimate glacial terminations.** **a**, CO<sub>2</sub> from Vostok<sup>47</sup> (TII, brown) and EDC (ref. 49; TI, orange). **b**, δ<sup>13</sup>CH<sub>4</sub> from Vostok (TII, light blue), EDML (ref. 11; TI, purple, reprocessed and corrected for Kr effect) and GISP2 (ref. 13; TI, dark blue, original timescale, corrected for Kr effect), all with inverted y axis. **c**, CH<sub>4</sub> from EDC (ref. 7; TII, light green) and EDML (ref. 5; TI, dark green). Except for GISP2 δ<sup>13</sup>CH<sub>4</sub>, all records are given on the unified ice-core chronology<sup>46</sup>. Upper x axis refers to TI (0–25 kyr BP), lower x axis to TII (118–143 kyr BP), aligned at the major CH<sub>4</sub> rises (grey dotted line).

systems on tropical wetland emissions, fostered by a proportional scaling of emissions from the remaining non-geological CH<sub>4</sub> sources (mainly boreal wetlands and biomass burning), combined with a slight change in CH<sub>4</sub> lifetime during rapid climate change, represent the most likely explanation for strong CH<sub>4</sub> variability that is not accompanied by synchronous δ<sup>13</sup>CH<sub>4</sub> changes.

### Climate and CO<sub>2</sub>-induced changes in wetland ecosystems

The time interval between 71 and 65 kyr BP in our δ<sup>13</sup>CH<sub>4</sub> record (the MIS 5–4 transition), particularly, demonstrates the decoupling of changes in δ<sup>13</sup>CH<sub>4</sub> from atmospheric CH<sub>4</sub> mixing ratios, which were rather stable at that time (~450 ppb). CH<sub>4</sub> variations did not exceed 50 ppb, whereas δ<sup>13</sup>CH<sub>4</sub> shifted strongly (~4‰) towards higher values. At the same time sea level dropped by 30–40 m and CO<sub>2</sub> levels decreased by 35 ppm leading to boundary conditions comparable to glacial maxima.

We can think of two plausible explanations that would account for δ<sup>13</sup>CH<sub>4</sub> variations during periods of relatively constant CH<sub>4</sub> concentrations. First, there could be periods when one source with low δ<sup>13</sup>CH<sub>4</sub> was replaced by an equivalent increase in a source with an increased δ<sup>13</sup>CH<sub>4</sub> signature, causing a net shift in the mean isotopic composition, while keeping the overall CH<sub>4</sub> loading constant. For example, the progressive glaciation of high-latitude Northern Hemisphere land masses was probably accompanied by a significant reduction of <sup>13</sup>C-depleted boreal methane sources<sup>6,18,31</sup>. The CH<sub>4</sub> load could be maintained by the increase of tropical emissions, for example, related to the expansion of tropical wetland sources on newly exposed shelf areas such as the Sunda shelf<sup>31</sup>. Assuming a 10‰ difference in their δ<sup>13</sup>CH<sub>4</sub> signature, shifting 30 Tg CH<sub>4</sub> yr<sup>-1</sup> from boreal to tropical wetland emissions could explain

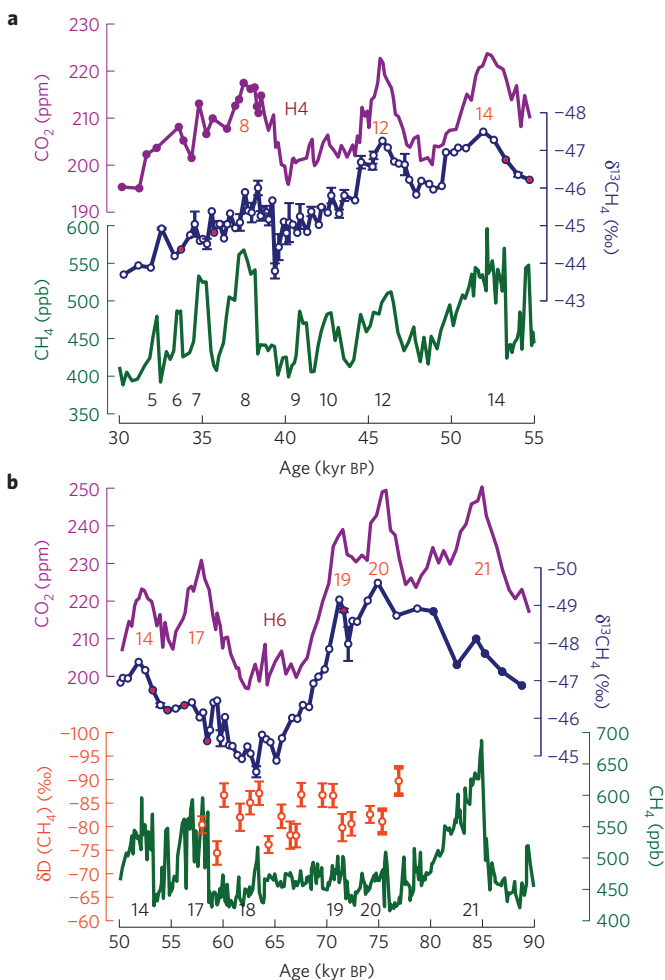


**Figure 3 | Zoom into MIS 3 and the MIS 5–4 boundary.** **a**, CO<sub>2</sub> between 30 and 55 kyr BP from EDML and Talos Dome<sup>48</sup> (purple), after 38.5 kyr BP from Byrd<sup>14</sup> (filled circles). δ<sup>13</sup>CH<sub>4</sub> from EDML (blue) and CH<sub>4</sub> from EDML (ref. 5; green). **b**, CO<sub>2</sub> from EDML and Talos Dome<sup>48</sup> (purple) between 50 and 90 kyr BP. Composite δ<sup>13</sup>CH<sub>4</sub> (blue) (80–90 kyr BP from Vostok (filled circles), all others from EDML (open circles), y axis inverted). Samples potentially subject to diffusive fractionation marked by red circle fillings. δD(CH<sub>4</sub>) from EDML (orange), CH<sub>4</sub> from EDML (ref. 5; green). H numbers indicate the timing of Heinrich events in the North Atlantic. Arabic numbers indicate the timing of Dansgaard–Oeschger events and their respective Antarctic counterparts<sup>12</sup>. All data sets are reported on the unified ice-core chronology<sup>46</sup>. Standard deviations of replicate measurements illustrated by error bars.

an atmospheric increase of 2‰ in δ<sup>13</sup>CH<sub>4</sub>. Note that this would also imply a near shutdown of all boreal sources.

To investigate whether such a shift occurred during the MIS 5–4 transition, we also measured δD(CH<sub>4</sub>) over this interval (Fig. 3b). At first order, δD(CH<sub>4</sub>) is a function of the hydrogen isotopic signature of the precipitation in wetland areas<sup>12,28</sup>. Accordingly, we would expect a general increase in δD(CH<sub>4</sub>) values to accompany the observed δ<sup>13</sup>CH<sub>4</sub> shift, if boreal CH<sub>4</sub> sources were exchanged with tropical sources, which are more enriched in deuterium. However, our complementary δD(CH<sub>4</sub>) data do not show such a covariation, indicating that a simple exchange of one source for another cannot satisfactorily explain the observed δ<sup>13</sup>CH<sub>4</sub> enrichment. Note that a large change in the hydrogen isotopic signature of boreal wetlands expected for cold conditions<sup>32</sup> would not have had a strong influence on the atmospheric composition if boreal wetland emissions were already low before the MIS 5–4

transition<sup>31</sup>. This hypothesis would lend support to the idea that  $\delta^{13}\text{CH}_4$  is governed mainly by processes taking place in the tropics at that time.

Another, more likely, explanation for the  $\delta^{13}\text{CH}_4$  shift during the MIS 5–4 transition involves changes in the characteristic isotope values of individual sources themselves<sup>33</sup>, controlled by climate and  $\text{CO}_2$ -induced changes in ecosystem composition. As the primary process of  $\text{CH}_4$  production is the anaerobic decomposition of plant material, atmospheric  $\text{CO}_2$  affects  $\delta^{13}\text{CH}_4$  in many ways. Changes in the carbon isotopic signature of  $\text{CO}_2$  ( $\delta^{13}\text{CO}_2$ ) are directly imprinted in  $\delta^{13}\text{CH}_4$  through incorporation into the plant precursor material during photosynthesis. However, the  $\delta^{13}\text{CO}_2$  variations over glacial–interglacial cycles (0.2–0.5‰) are small<sup>34</sup> compared with those in  $\delta^{13}\text{CH}_4$ . More notably, the  $\text{CO}_2$  concentration itself may have an impact on  $\delta^{13}\text{CH}_4$  in two ways.

First,  $\text{CO}_2$  influences the C3/C4 plant ratio, with the relatively  $^{13}\text{C}$ -enriched C4 large subscript for all mentions of C3 and C4 plants as in <http://www.nature.com/nggeo/journal/v6/n8/full/ngeo1856.html> plants being favoured under glacial, low- $\text{CO}_2$  conditions<sup>35–37</sup>. The effect of this C3/C4 plant shift on  $\delta^{13}\text{CH}_4$  has been estimated to be about 0.7‰ (ref. 33). This estimate, however, is a lower limit as it was based on the direct competition of C3 and C4 grasses for prescribed grassland areas derived from a modern vegetation map<sup>38</sup>. Taking an extension of grasslands under glacial conditions into account<sup>36,37,39</sup>, we expect a significantly stronger effect. The weight of  $\text{CO}_2$  variability for the isotopic signature of plant precursor material is also indicated by the striking correlation between  $\text{CO}_2$  and  $\delta^{13}\text{CH}_4$  over the entire 160 kyr period. Pronounced deviations in this correlation occur immediately after some abrupt increase in  $\text{CH}_4$  (that is, Dansgaard–Oeschger events 17, 21, 24 and the onsets of both interglacials, Fig. 1). Note that each of these intervals is preceded by a significant increase in sea level<sup>3,4</sup>, which would have flooded low-lying coastal regions. This implies that changes in the source signature do not follow a simple one-to-one relationship with  $\text{CO}_2$ , but that  $\delta^{13}\text{CH}_4$  is most likely a convoluted signal of wetland area and ecosystem response.

Second, a further effect on  $\delta^{13}\text{CH}_4$  is caused by the change of the isotopic signature of C3 vegetation, linked to a change in isotopic fractionation during  $\text{CO}_2$  uptake<sup>39</sup>. Differences in the range of 3–4‰ are reported in C3 plant materials in equatorial Africa between rainforest habitats on the one extreme and open savanna-type habitats on the other<sup>40</sup>. Accordingly, a shift from forest- and rainforest-type ecosystems during interglacial conditions to seasonally inundated savanna-type ecosystems during the glacial would also lead to  $\text{CH}_4$  emissions increasingly enriched in  $^{13}\text{C}$  during the MIS 5–4 transition.

Indicative evidence for such ecosystem changes may be found in coastal marine sediment records. For example,  $\delta^{13}\text{C}$  of plant biomarkers in sediment cores off the East Atlantic coast close to the river mouths of the Congo and Angola basins indicate 3–4‰ higher values during glacial times<sup>41</sup>, similar to evidence from the Guinea Plateau margin recording Sahara/Sahel vegetation<sup>42</sup>. A comparable marine geological study from the Cariaco Basin in the tropical West Atlantic reported a 4–5‰  $\delta^{13}\text{C}$  decrease in leaf waxes from the Last Glacial Maximum (LGM) to the preboreal Holocene<sup>43</sup>. We acknowledge that such signature changes may reflect vegetation shifts only in river catchment areas. Furthermore, it remains unclear whether changes in atmospheric  $\text{CO}_2$  exert a similar influence on  $\delta^{13}\text{C}$  of plant material in permanent wetlands. However, we assume that during generally drier glacial conditions an even larger part of tropical  $\text{CH}_4$  emissions are caused by seasonally inundated flood plains<sup>44</sup> whose vegetation is controlled by the postulated influence of climate and  $\text{CO}_2$  on the carbon isotope composition of the plant precursor material. Moreover, shifts in the isotopic signature of such seasonal wetland ecosystems would also be documented in coastal marine sediment records through riverine transport.

Considering the still insufficient understanding of the factors controlling ecosystem composition and  $\text{CH}_4$  emissions, a definitive quantification of the combined effects of shifts in the C3/C4 plant ratio and changes in the C3 plant isotopic signature on low-latitude  $\delta^{13}\text{CH}_4$  seems to be premature. Our estimates show that none of the proposed processes discussed above is likely to explain the full range of observed  $\delta^{13}\text{CH}_4$  changes over the MIS 5–4 transition ( $\sim 4\text{‰}$ ) or even over the full glacial sequence ( $\sim 8\text{‰}$ ). However, the sum of the individual processes together with changes in the ratio of net to gross production of  $\text{CH}_4$  in wetlands<sup>28</sup> lie well within the range of the observed  $\delta^{13}\text{CH}_4$  changes. We stress that, except for a change in net to gross production of  $\text{CH}_4$ , all these effects are neutral with respect to  $\delta\text{D}(\text{CH}_4)$ , in line with our results. In essence, a change in the carbon isotopic signature of  $\text{CH}_4$  from tropical, seasonally inundated floodplains controlled by changing climate and  $\text{CO}_2$  conditions, seems to be an essential ingredient to explain the large changes in  $\delta^{13}\text{CH}_4$  at times when  $\text{CH}_4$  concentrations remained rather constant.

### Implications for glacial–interglacial $\text{CH}_4$ changes

The conclusions above encourage a reinterpretation of the changes over the past glacial–interglacial transition. In previous work<sup>11</sup>, we proposed changes in the source mix to explain  $\text{CH}_4$  changes over termination I, where we kept the isotopic signatures of individual sources essentially constant. A close look at the evolution of  $\text{CH}_4$  and  $\delta^{13}\text{CH}_4$  during the transition indicates that only the 1.1‰ depletion of  $\delta^{13}\text{CH}_4$  into the Bølling–Allerød is synchronous with a concurrent steep  $\text{CH}_4$  rise of about 150 ppb (Fig. 2), whereas the rapid Younger Dryas—Preboreal Holocene transition exhibits a more gradual change in  $\delta^{13}\text{CH}_4$ . A decoupling of  $\delta^{13}\text{CH}_4$  and  $\text{CH}_4$  thus also applies for the rapid  $\text{CH}_4$  changes during termination I. Similar to the strong increase in  $\delta^{13}\text{CH}_4$  during the MIS 5–4 transition, at least part of the deglacial  $\delta^{13}\text{CH}_4$  decrease during termination I could alternatively be attributed to a progressive depletion of the isotopic signature of  $\text{CH}_4$  sources. Such a depletion in  $\delta^{13}\text{CH}_4$  source signatures from the LGM to the Holocene would also have a pronounced effect on the change in the source mix required to explain the  $\text{CH}_4$  changes. For example, our previous box model approach assumed temporally constant wetland isotopic signatures over the past 25 kyr leading to comparable wildfire  $\text{CH}_4$  emissions for the LGM and the Holocene. However, if we increase the glacial  $\delta^{13}\text{CH}_4$  signature of tropical floodplains and biomass burning emissions owing to isotopic changes in the plant precursor material, much smaller wildfire emissions are required for the LGM to close the methane isotope budget. Accordingly, such a tropical source signature change would bring reconstructions of wildfire activity from charcoal records<sup>22,45</sup> and  $\delta^{13}\text{CH}_4$  into closer agreement.

The expanded database of  $\delta^{13}\text{CH}_4$  variations over the past glacial cycle presented here provides unique information on unexpected changes in the  $\text{CH}_4$  source regions. Fast methane concentration rises at Dansgaard–Oeschger warmings and during the deglaciations do not seem to be driven by large relative source or sink mix changes, or by activation of northern high-latitude sources alone. Rather, the new isotopic data constraints suggest that glacial changes in atmospheric  $\text{CH}_4$  and  $\delta^{13}\text{CH}_4$  are related to a predominant tropical wetland source, which responded quickly to Dansgaard–Oeschger climate variability and associated changes in the hydrological cycles. Scaling of other non-geological sources, as well as emission feedbacks on atmospheric  $\text{CH}_4$  lifetimes, probably contributed to major  $\text{CH}_4$  changes, but were in most cases either neutral with regard to  $\delta^{13}\text{CH}_4$  or of lesser importance.

Our new data provide strong evidence that shifts in the isotopic signature of tropical floodplain emissions could be the main driver of  $\delta^{13}\text{CH}_4$  variability, especially in glacial periods.  $\delta^{13}\text{CH}_4$  changes are probably modulated by feedbacks of climate and atmospheric

CO<sub>2</sub> on the composition of wetland ecosystems in the low latitudes. Quantifying individual source and sink contributions to the glacial δ<sup>13</sup>CH<sub>4</sub> changes will remain elusive until the uncertainties in source and sink variability are reduced. Further high-resolution studies of δD(CH<sub>4</sub>) could complement the data presented here, but a deeper understanding of wetland dynamics and vegetation shifts is also required and should be implemented in CH<sub>4</sub> emission schemes in dynamic vegetation models.

## Methods

We reconstructed atmospheric δ<sup>13</sup>CH<sub>4</sub> records using wet extraction techniques and continuous flow gas chromatography combustion isotope ratio mass spectrometry (GC/C/IRMS) measurements carried out on ice-core material from both the European Project for Ice Coring in Antarctica (EPICA) core from Dronning Maud Land (EDML) and the Vostok cores. At the Alfred Wegener Institute we analysed 151 samples from the EDML core (including 32 replicates, reproducibility of 0.2‰, 1σ) to construct a high-resolution record between 20 and 75 kyr BP with an average temporal resolution of better than one sample every 500 years. The period covering the two most pronounced climatic excursions in the Greenland temperature record during MIS 3 (Dansgaard–Oeschger events 7 and 8) were sampled with a resolution of ~200 years. A complementary record of 79 samples of Vostok ice-core material covering a time period from 50 to 160 kyr BP was measured at the Pennsylvania State University with an analytical uncertainty of 0.3‰ (1σ), equivalent to an average temporal resolution of 1,660 years. Both data sets overlap well between 50 and 75 kyr BP, suggesting the spliced record is likely to be a good representation of the true atmospheric record between 20 and 160 kyr BP. The two records were corrected for instrumental interference from atmospheric krypton, for gravitational settling in the firn and for a minor interlaboratory offset of 0.14‰. Owing to the uncertainties concerning firn transport characteristics at the core sites under glacial conditions and the exact timings of the onsets of relevant rapid CH<sub>4</sub> increases, we did not apply a general correction for diffusive fractionation. The largest CH<sub>4</sub> rises are estimated to cause δ<sup>13</sup>C shifts in the range of 0.6–1.0‰. We marked those seven δ<sup>13</sup>CH<sub>4</sub> samples that are potentially affected by diffusive fractionation in the respective figures to illustrate their limited reliability. All δ<sup>13</sup>C values are reported versus Vienna PeeDee Belemnite.

We further analysed 20 samples of EDML ice for δD(CH<sub>4</sub>) with an external precision of about 2.5‰ (1σ). The measurements were carried out at the University of Bern using a purge and trap extraction coupled to a gas chromatography pyrolysis isotope ratio mass spectrometer (GC/P/IRMS) and cover the MIS 5–4 transition with an average resolution of 1.5 kyr in between 54 and 85 kyr BP. The δD(CH<sub>4</sub>) values are reported with respect to the international Vienna Standard Mean Ocean Water scale.

The δ<sup>13</sup>CH<sub>4</sub> and δD(CH<sub>4</sub>) records are dated according to the unified Antarctic ice-core chronology<sup>46</sup>. For additional details on the chronology, analytical methods, correction procedures and corresponding references, please refer to the Supplementary Information.

**Data.** All data are available at [www.pangaea.de](http://www.pangaea.de) (<http://doi.pangaea.de/10.1594/PANGAEA.812116>) and in the NOAA/World Data Center for Paleoclimatology archive ([http://hurrricane.ncdc.noaa.gov/pls/paleox/f?p=519:1:::1\\_P1\\_STUDY\\_ID:14651](http://hurrricane.ncdc.noaa.gov/pls/paleox/f?p=519:1:::1_P1_STUDY_ID:14651))

Received 8 March 2013; accepted 18 July 2013; published online 25 August 2013

## References

- North GRIP members, High-resolution record of Northern Hemisphere climate extending into the last interglacial period. *Nature* **431**, 147–151 (2004).
- EPICA community members, One-to-one coupling of glacial climate variability in Greenland and Antarctica. *Nature* **444**, 195–198 (2006).
- Rohling, E. J. *et al.* Antarctic temperature and global sea level closely coupled over the past five glacial cycles. *Nature Geosci.* **2**, 500–504 (2009).
- Grant, K. M. *et al.* Rapid coupling between ice volume and polar temperature over the past 150,000 years. *Nature* **491**, 744–747 (2012).
- Schilt, A. *et al.* Atmospheric nitrous oxide during the last 140,000 years. *Earth Planet. Sci. Lett.* **300**, 33–43 (2010).
- Chappellaz, J. *et al.* Synchronous changes in atmospheric CH<sub>4</sub> and Greenland climate between 40 and 8 kyr BP. *Nature* **366**, 443–445 (1993).
- Loulergue, L. *et al.* Orbital and millennial-scale features of atmospheric CH<sub>4</sub> over the past 800,000 years. *Nature* **453**, 383–386 (2008).
- Brook, E. J., Harder, S., Severinghaus, J., Steig, E. J. & Sucher, C. M. On the origin and timing of rapid changes in atmospheric methane during the last glacial period. *Glob. Biogeochem. Cycles* **14**, 559–572 (2000).
- Dällenbach, A. *et al.* Changes in the atmospheric CH<sub>4</sub> gradient between Greenland and Antarctica during the last glacial and the transition to the holocene. *Geophys. Res. Lett.* **27**, 1005–1008 (2000).
- Baumgartner, M. *et al.* High-resolution inter-polar difference of atmospheric methane around the Last Glacial Maximum. *Biogeosci. Discuss.* **9**, 5471–5508 (2012).
- Fischer, H. *et al.* Changing boreal methane sources and constant biomass burning during the last termination. *Nature* **452**, 864–867 (2008).
- Bock, M. *et al.* Hydrogen isotopes preclude marine hydrate CH<sub>4</sub> emissions at the onset of Dansgaard–Oeschger events. *Science* **328**, 1686–1689 (2010).
- Sowers, T. Atmospheric methane isotope records covering the Holocene period. *Quat. Sci. Rev.* **29**, 213–221 (2010).
- Ahn, J. & Brook, E. J. Atmospheric CO<sub>2</sub> and climate on Millennial time scales during the last glacial period. *Science* **322**, 83–85 (2008).
- Whiticar, M. & Schaefer, H. Constraining past global tropospheric methane budgets with carbon and hydrogen isotope ratios in ice. *Phil. Tran. R. Soc. A* **365**, 1793–1828 (2007).
- Hopcroft, P. O., Valdes, P. J. & Beerling, D. J. Simulating idealized Dansgaard–Oeschger events and their potential impacts on the global methane cycle. *Quat. Sci. Rev.* **30**, 3258–3268 (2011).
- Levine, J. G. *et al.* Reconciling the changes in atmospheric methane sources and sinks between the Last Glacial Maximum and the pre-industrial era. *Geophys. Res. Lett.* **38**, L23804 (2011).
- Brook, E. J., Sowers, T. & Orchardo, J. Rapid variations in atmospheric methane concentration during the past 110,000 years. *Science* **273**, 1087–1091 (1996).
- Wang, X. *et al.* Wet periods in northeastern Brazil over the past 210 kyr linked to distant climate anomalies. *Nature* **432**, 740–743 (2004).
- Peterson, L. C. & Haug, G. H. Variability in the mean latitude of the Atlantic Intertropical Convergence Zone as recorded by riverine input of sediments to the Cariaco Basin (Venezuela). *Palaeogeogr. Palaeoclimatol. Palaeoecol.* **234**, 97–113 (2006).
- Wang, Y. *et al.* Millennial- and orbital-scale changes in the East Asian monsoon over the past 224,000 years. *Nature* **451**, 1090–1093 (2008).
- Daniau, A.-L., Harrison, S. & Bartlein, P. Fire regimes during the Last Glacial. *Quat. Sci. Rev.* **29**, 2918–2930 (2010).
- Zimov, S. A. *et al.* North Siberian lakes: A methane source fueled by pleistocene carbon. *Science* **277**, 800–802 (1997).
- Walter, K. M., Edwards, M. E., Grosse, G., Zimov, S. A. & Chapin, F. S., I. Thermokarst lakes as a source of atmospheric CH<sub>4</sub> during the last deglaciation. *Science* **318**, 633–636 (2007).
- Judd, A. G., Hovland, M., Dimitrov, L. I., García Gil, S. & Jukes, V. The geological methane budget at Continental Margins and its influence on climate change. *Geofluids* **2**, 109–126 (2002).
- Luyendyk, B., Kennett, J. & Clark, J. F. Hypothesis for increased atmospheric methane input from hydrocarbon seeps on exposed continental shelves during glacial low sea level. *Mar. Petrol. Geol.* **22**, 591–596 (2005).
- Kennett, J. P., Cannariato, K. G., Hendy, I. L. & Behl, R. J. Carbon isotopic evidence for methane hydrate instability during quaternary interstadials. *Science* **288**, 128–133 (2000).
- Sowers, T. Late quaternary atmospheric CH<sub>4</sub> isotope record suggests marine clathrates are stable. *Science* **311**, 838–840 (2006).
- Valdes, P. J., Beerling, D. J. & Johnson, C. E. The ice age methane budget. *Geophys. Res. Lett.* **32**, L02704 (2005).
- Kaplan, J. O., Folberth, G. & Hauglustaine, D. A. Role of methane and biogenic volatile organic compound sources in late glacial and Holocene fluctuations of atmospheric methane concentrations. *Glob. Biogeochem. Cycles* **20**, GB2016 (2006).
- Weber, S. L., Drury, A. J., Toonen, W. H. J. & van Weele, M. Wetland methane emissions during the Last Glacial Maximum estimated from PMIP2 simulations: Climate, vegetation, and geographic controls. *J. Geophys. Res.* **115**, D06111 (2010).
- Jouzel, J., Hoffmann, G., Koster, R. & Masson, V. Water isotopes in precipitation: Data/model comparison for present-day and past climates. *Quat. Sci. Rev.* **19**, 363–379 (2000).
- Schaefer, H. & Whiticar, M. J. Potential glacial–interglacial changes in stable carbon isotope ratios of methane sources and sink fractionation. *Glob. Biogeochem. Cycles* **22**, GB1001 (2008).
- Schmitt, J. *et al.* Carbon isotope constraints on the deglacial CO<sub>2</sub> rise from Ice Cores. *Science* **336**, 711–714 (2012).
- Ehleringer, J. R., Cerling, T. E. & Helliker, B. R. C4 photosynthesis, atmospheric CO<sub>2</sub>, and climate. *Oecologia* **112**, 285–299 (1997).
- Harrison, S. P. & Prentice, C. I. Climate and CO<sub>2</sub> controls on global vegetation distribution at the last glacial maximum: Analysis based on palaeovegetation data, biome modelling and palaeoclimate simulations. *Glob. Change Biol.* **9**, 983–1004 (2003).
- Bragg, F. J. *et al.* Stable isotope and modelling evidence for CO<sub>2</sub> as a driver of glacial–interglacial vegetation shifts in southern Africa. *Biogeosciences* **10**, 2001–2010 (2013).
- Collatz, G. J., Berry, J. A. & Clark, J. S. Effects of climate and atmospheric CO<sub>2</sub> partial pressure on the global distribution of C4 grasses: Present, past, and future. *Oecologia* **114**, 441–454 (1998).

39. Kaplan, J. O., Prentice, I. C., Knorr, W. & Valdes, P. J. Modeling the dynamics of terrestrial carbon storage since the Last Glacial Maximum. *Geophys. Res. Lett.* **29**, 31-1–31-4 (2002).
40. Vogts, A., Moossen, H., Rommerskirchen, F. & Rullkötter, J. Distribution patterns and stable carbon isotopic composition of alkanes and alkan-1-ols from plant waxes of African rain forest and savanna C3 species. *Org. Geochem.* **40**, 1037–1054 (2009).
41. Rommerskirchen, F., Eglinton, G., Dupont, L. & Rullkötter, J. Glacial/interglacial changes in southern Africa: Compound-specific  $\delta^{13}\text{C}$  land plant biomarker and pollen records from southeast Atlantic continental margin sediments. *Geochem. Geophys. Geosyst.* **7**, Q08010 (2006).
42. Castañeda, I. S. *et al.* Wet phases in the Sahara/Sahel region and human migration patterns in North Africa. *Proc. Natl Acad. Sci. USA* **106**, 20159–20163 (2009).
43. Huguen, K. A., Eglinton, T. I., Xu, L. & Makou, M. Abrupt tropical vegetation response to rapid climate changes. *Science* **304**, 1955–1959 (2004).
44. Mitsch, W. *et al.* Tropical wetlands: Seasonal hydrologic pulsing, carbon sequestration, and methane emissions. *Wetlands Ecol. Manage.* **18**, 573–586 (2010).
45. Marlon, J. R. *et al.* Wildfire responses to abrupt climate change in North America. *Proc. Natl Acad. Sci. USA* **106**, 2519–2524 (2009).
46. Lemieux-Dudon, B. *et al.* Consistent dating for Antarctic and Greenland ice cores. *Quat. Sci. Rev.* **29**, 8–20 (2010).
47. Petit, J. R. *et al.* Climate and atmospheric history of the past 420,000 years from the Vostok ice core, Antarctica. *Nature* **399**, 429–436 (1999).
48. Bereiter, B. *et al.* Mode change of millennial  $\text{CO}_2$  variability during the last glacial cycle associated with a bipolar marine carbon seesaw. *Proc. Natl Acad. Sci. USA* **109**, 9755–9760 (2012).
49. Monnin, E. *et al.* Atmospheric  $\text{CO}_2$  concentrations over the last glacial termination. *Science* **291**, 112–114 (2001).
50. EPICA community members, Eight glacial cycles from an Antarctic ice core. *Nature* **429**, 623–628 (2004).

### Acknowledgements

This work is a contribution to the EPICA; a joint ESF/EC scientific programme, financially supported by the EC and by national contributions from Belgium, Denmark, France, Germany, Italy, The Netherlands, Norway, Sweden, Switzerland and the United Kingdom. This is EPICA publication no. 293. Financial support for this work has been provided in part by the European Research Council Advanced Grant MATRICs, Schweizerischer Nationalfonds and Deutsche Forschungsgemeinschaft, and is also a contribution to the European Union's Seventh Framework programme (FP7/2007-2013, grant no. 243908), 'Past4Future. Climate Change: Learning from the past climate'. This is Past4Future contribution no. 55. Financial support for T.S. was derived from NSF grants 09-44584 and 09-68391.

### Author contributions

L.M., T.S., M. Bock and M. Behrens carried out the measurements. R.S. modelled the diffusion fractionation in the firn column. L.M. and H.F. wrote the manuscript. All authors worked on the scientific interpretation, contributed to the discussion with ideas and comments or helped to review the manuscript.

### Additional information

Supplementary information is available in the [online version of the paper](#). Reprints and permissions information is available online at [www.nature.com/reprints](http://www.nature.com/reprints). Correspondence and requests for materials should be addressed to H.F.

### Competing financial interests

The authors declare no competing financial interests.